

PAPER

Cosmic ray ensembles as signatures of ultra-high energy photons interacting with the solar magnetic field

To cite this article: The CREDO collaboration *et al* JCAP03(2022)038

View the [article online](#) for updates and enhancements.

You may also like

- [Contemporary processes and the selection of materials in historical urban greenery areas on example from Cracow and Warsaw](#)
Wojciech Bobek and Katarzyna Lakomy
- [Recreational and Tourist Qualities of Submontane Resorts Within the Cracow Metropolitan Area](#)
Hanna Hrehorowicz – Gaber
- [Loss of Potential: Large-Panel Housing Estates – Czyżyny Case](#)
Eliza Szczerek



IOP | ebooks™

Bringing together innovative digital publishing with leading authors from the global scientific community.

Start exploring the collection—download the first chapter of every title for free.

Cosmic ray ensembles as signatures of ultra-high energy photons interacting with the solar magnetic field



The CREDO collaboration

N. Dhital,^{a,b} P. Homola,^b D. Alvarez-Castillo,^{b,c} D. Góra,^b
H. Wilczyński,^b K. Almeida Cheminant,^b B. Poncyljusz,^d
J. Mędrala,^e G. Opiła,^e A. Bhatt,^a B. Łozowski,^f G. Bhatta,^b
Ł. Bibrzycki,^g T. Bretz,^h A. Ćwikła,ⁱ L. Del Peral,^j A.R. Duffy,^k
A.C. Gupta,^l B. Hnatyk,^m P. Jagoda,^{e,b} M. Kasztelan,ⁿ
K. Kopański,^b P. Kovacs,^o M. Krupinski,^b M. Medvedev,^{p,q}
V. Nazari,^c M. Niedźwiecki,^r D. Ostrogórski,^e M. Piekarczyk,^g
M.D. Rodríguez Frías,^j K. Rzecki,^e K. Smelcerz,ⁱ K. Smolek,^s
J. Stasielak,^b O. Sushchov,^b T. Wibig,^t K. Wozniak,^b
J. Zamora-Saa,^{u,v} Z. Zimborás^o and A. Tursunov^w

^aCentral Department of Physics, Tribhuvan University,
Kirtipur, Kathmandu 44613, Nepal

^bInstitute of Nuclear Physics PAN,
ul. Radzikowskiego 152, Cracow 31-342, Poland

^cJoint Institute for Nuclear Research,
6 Joliot-Curie St, Dubna 141980, Russia

^dFaculty of Physics, University of Warsaw,
ul. Pasteura 5, Warsaw 02-093, Poland

^eFaculty of Physics and Computer Science, AGH University of Science and Technology,
Cracow 30-059, Poland

^fFaculty of Natural Sciences, University of Silesia in Katowice,
Bankowa 9, Katowice 40-007, Poland

^gPedagogical University of Cracow,
Podchorążych 2, Cracow 30-084, Poland

^hPhysics Institute III A, RWTH Aachen University,
Otto-Blumenthal-Straße, Aachen 52074, Germany

ⁱDepartment of Computer Science, Faculty of Computer Science and Telecommunications,
Cracow University of Technology,
Warszawska Street 24, Cracow 31-155, Poland

^jDepartment of Physics and Mathematics, University of Alcalá,
Pza. San Diego, s/n, Alcalá de Henares, Madrid 28801, Spain

^kCentre for Astrophysics and Supercomputing, Swinburne University of Technology,
John St, Hawthorn, VIC 3122, Australia

^lAryabhata Research Institute of Observational Sciences (ARIES),
Manora Peak, Nainital 263001, Uttarakhand, India

^mAstronomical Observatory of Taras Shevchenko National University of Kyiv,
Observatorna str. 3, Kyiv 04053, Ukraine

ⁿNational Centre for Nuclear Research,
ul. Andrzeja Sołtana 7, Otwock-Swierk 05-400, Poland

^oInstitute for Particle and Nuclear Physics, Wigner Research Centre for Physics,
Konkoly-Thege Miklós út 29-33, Budapest 1121, Hungary

^pDepartment of Physics and Astronomy, Kansas University,
Malott Hall, Room 1082, 1251 Wescoe Hall Drive, Lawrence, KS 66045, U.S.A.

^qLaboratory for Nuclear Science, Massachusetts Institute of Technology,
77 Massachusetts Ave, Cambridge, MA 02139, U.S.A.

^rInstitute of Telecomputing, Faculty of Physics, Mathematics and Computer Science,
Cracow University of Technology,
Warszawska Street 24, Cracow 31-155, Poland

^sInstitute of Experimental and Applied Physics, Czech Technical University in Prague,
Husova 240/5 Prague 1, Prague 110 00, Czech Republic

^tUniversity of Łódź, Faculty of Physics and Applied Informatics,
ul. Pomorska 149/153, Łódź 90-236, Poland

^uCenter for Theoretical and Experimental Particle Physics (CTEPP),
Facultad de Ciencias Exactas, Universidad Andrés Bello, Departamento de Ciencias Físicas,
Avenida Republica 498, Santiago 8370146, Chile

^vMillennium Institute for Subatomic Physics at High Energy Frontier — SAPHIR,
Fernandez Concha 700, Santiago 7591538, Chile

^wResearch Centre for Theoretical Physics and Astrophysics, Institute of Physics,
Silesian University in Opava,
Bezručovo nám. 13, Opava CZ-74601, Czech Republic

E-mail: dalvarez@ifj.edu.pl

Received November 18, 2021

Accepted February 4, 2022

Published March 16, 2022

Abstract. Propagation of ultra-high energy photons in the solar magnetosphere gives rise to cascades comprising thousands of photons. We study the cascade development using Monte Carlo simulations and find that the photons in the cascades are spatially extended over millions of kilometers on the plane distant from the Sun by 1 AU. We estimate the chance of detection considering upper limits from current cosmic rays observatories in order to provide

an optimistic estimate rate of 0.002 events per year from a chosen ring-shaped region around the Sun. We compare results from simulations which use two models of the solar magnetic field, and show that although signatures of such cascades are different for the models used, for practical detection purpose in the ground-based detectors, they are similar.

Keywords: cosmic ray experiments, cosmic ray theory, cosmic rays detectors, ultra high energy cosmic rays

ArXiv ePrint: [1811.10334](https://arxiv.org/abs/1811.10334)

Contents

1	Introduction	1
2	Simulation	2
3	Results	5
3.1	Multi air shower footprints at the ground level	6
4	Summary and prospects	13

1 Introduction

Detection of ultra-high energy (UHE) photons, that bear energies of EeV and beyond, will have a significant impact on the understanding of fundamental science. As an example, dark matter (DM) searches up to the electroweak scale (~ 100 GeV) so far have not been able to produce conclusive evidence of DM particles [1–3]. For this reason, it becomes even more important to explore the mass regimes corresponding to the other natural scales — the GUT ($\sim 10^{16}$ GeV) and the Planck ($\sim 10^{19}$ GeV) scales for potential DM candidates [4, 5]. A common method in the DM search has been the indirect search, which relies on the detection of products of DM particle decay and annihilation. Various proposed models of particle interactions predict that products of such interactions consist of UHE photons and standard model (SM) particles with a possibility of other elementary particles which do not fit into the SM [6]. Detection of UHE photons will also help substantiate the Greisen-Zatsepin-Kuzmin (GZK) effect, a steepening of cosmic ray energy spectrum around 4×10^{19} eV as a consequence of interaction of UHE cosmic rays (UHECRs) with cosmic microwave background radiation [7, 8]. Widely used techniques of UHE photon detection rely on two main approaches; first, analyses based on parameters (e.g., the depth of maximum development of an extensive air shower, X_{\max}) from the reconstructed longitudinal profiles of development of extensive air showers (EASs) initiated by UHE photons [11], and the other based on observables derived from signal recorded by ground-based detector arrays from the secondary particles of EASs [12]. In principle, both approaches should be able to distinguish between photon- and hadron-initiated showers. The photon-initiated showers are expected to have deeper X_{\max} compared to the hadron-initiated ones, and the particle contents for the two types of showers are expected to be different — hadronic showers being more muon-rich than the other. The most up-to-date results from searches implementing these techniques have reported not only the non-observation of (significant) photon candidates in UHECR data,

thus enabling us to place stringent upper limits on UHE photon fraction (flux) [9–12], but also the observation of an excess of muons in data compared to what one would expect from simulations of hadronic showers [13, 14]. Given such a discrepancy between the measurements and the results from simulations of hadronic showers, which is possibly due to the lack of complete understanding of the physics at the UHE regime, it is very appealing to revisit also the UHE photon scenario but with a different approach.

The alternative approach presented in this paper is based on the electromagnetic cascading of UHE photons traversing regions nearby the Sun. Simulation results from a study of such a cascading process were presented in [15], which give an expected size of a footprint of core part of the cascade at the top of the Earth’s atmosphere. The footprint is expected to be a highly prolate ellipse with a size of the order of a few kilometers. In our simulations, we take into account the more accurate physics of cascade development and tracking of the cascade particles so that we are able to characterize the particle distribution better. The cascading process starts when a UHE photon experiences solar magnetic field component transverse to the direction of its trajectory sufficiently large for magnetic pair production. The electron-positron pairs thus produced undergo a magnetic bremsstrahlung process and emit photons as they propagate in the magnetic field. Also, among the emitted photons, those with sufficiently high energy will undergo magnetic pair production and repeat the process. As a consequence, a cascade comprising several thousand photons and several e^+e^- develops in the region nearby the Sun. Although deflections suffered by the e^+e^- during their propagation are very small when considered only within these regions, they give rise to an extended spatial distribution of cascade particles after propagating through the Sun-Earth distance ($\sim 1.5 \times 10^{11}$ m). For UHE photons heading towards the Earth through the regions in the Sun’s vicinity, a unique particle distribution is expected as the cascade reaches the Earth. Such a cascading of UHE photons can occur even in the presence of the geomagnetic field [16]. However, cascades produced in the geomagnetic field, which are called *preshowers*, comprise only few hundred particles and have very narrow spatial distribution (< 1 m). Due to this fact, they are practically indistinguishable from the cascades without the preshower effect unless they originate at much higher altitude or arrive at the Earth’s atmosphere at near horizontal direction. In the following part of this paper, we refer to the Sun-initiated cascades as *super-preshowers* (SPSs) in light of similar development mechanism as that of preshowers but with much larger number of secondary particles. For a recent review on the different aspects of SPSs and state-of-the-art studies we refer the reader to this work [17].

2 Simulation

The treatment of most of the physics processes involved in the simulation of SPS development has been adopted from the PRESHOWER program [16]. We have used the formalism for magnetic pair production from reference [18]. For n_{photons} UHE photons propagating through a magnetic field (H), the actual number of e^+e^- pairs produced (n_{pairs}) is given by,

$$n_{\text{pairs}} = n_{\text{photons}} \{1 - \exp[-\alpha(\chi) dl]\}, \quad (2.1)$$

where dl is the photon path length and $\alpha(\chi)$ is the photon attenuation coefficient, a function of parameter $\chi \equiv \frac{1}{2} \frac{h\nu}{m_e c^2} \frac{H}{H_{\text{cr}}}$, where $H_{\text{cr}} \equiv \frac{m_e^2 c^3}{e\hbar} = 4.414 \times 10^{13}$ G is the natural quantum-mechanical measure of magnetic field strength. In an ultra-relativistic limit, if $H \ll H_{\text{cr}}$, $\alpha(\chi)$ can be expressed as

$$\alpha(\chi) = \frac{1}{2} \frac{\alpha_{\text{em}}}{\lambda_c} \frac{H}{H_{\text{cr}}} T(\chi), \quad (2.2)$$

even millions of kilometers where λ_c is the Compton wavelength of the electron and $T(\chi)$ is a dimensionless auxiliary function which can be approximated by

$$T(\chi) \simeq \frac{0.16}{\chi} K_{1/3}^2 \left(\frac{2}{3\chi} \right), \quad (2.3)$$

and where $K_{1/3}$ is a modified Bessel function. Provided the path length under consideration (dl) is fairly small, eq. (2.1) can be expressed as a probability of conversion of UHE photon into e^+e^- pair (p_{conv}) within the interval dl . Thus, we have

$$p_{\text{conv}} = 1 - \exp(-\alpha(\chi) dl) \simeq \alpha(\chi) dl, \quad (2.4)$$

which for a much larger distance L takes the form,

$$P_{\text{conv}} = 1 - \exp \left[- \int_0^L \alpha(\chi) dl \right]. \quad (2.5)$$

The probability of conversion of a UHE photon into e^+e^- pair is evaluated using eq. (2.4). Also, a fraction of energy carried by a pair-member (ε) is chosen from the distribution

$$\frac{dn}{d\varepsilon} \approx \frac{\alpha_{\text{em}} H}{\lambda_c} \frac{\sqrt{3}}{9\pi\chi} \frac{[2 + \varepsilon(1 - \varepsilon)]}{\varepsilon(1 - \varepsilon)} K_{\frac{2}{3}} \left[\frac{1}{3\chi\varepsilon(1 - \varepsilon)} \right] \quad (2.6)$$

following [19].

As the conversion probability of UHE photons to e^+e^- pairs, their trajectories and characteristics of magnetic bremsstrahlung radiation emitted thereof depend on the magnetic field experienced by these particles along their trajectories, it is important that we incorporate a realistic solar magnetic field model in our simulation. Unsurprisingly, owing to the dynamic nature and complexity of the Sun's magnetic field, a model that can characterize the magnetic field completely is far from being achievable. Thus, we proceed first with a simple dipole model of solar magnetic field and later with another analytical model called the dipole-quadrupole-current-sheet (DQCS) model [20], see figure 1. For the dipole model, the magnetic moment of the dipole producing the field used in the simulation is $6.87 \times 10^{32} \text{ G} \cdot \text{cm}^3$. Although this is not a very realistic model, using it for the solar magnetic field in our simulations allows us to study the effects of orientation of considered dipole on the expected distribution of the particles in the SPS as they arrive at the top of the Earth's atmosphere. This will give us an idea of how the SPS development is affected by an evolution of solar magnetic field for example over a solar cycle. In addition, it serves for a comparison to the results obtained from the other model. The DQCS model on the other hand, is more realistic and gives a more reasonable magnetic field even in the interplanetary regions. Inclusion of this model in the simulation thus provides a more accurate tracking of e^+e^- on their way towards the Earth, and better treatment of magnetic bremsstrahlung processes.

We have introduced time and space tracking for particles in the cascade so that we obtain their arrival time distribution and lateral distribution as they reach the top of the Earth's atmosphere. Given a particle with kinetic energy E and charge q , propagating along the direction $\hat{\mathbf{v}}$ in a region defined by a magnetic field \mathbf{B} , the equation describing its motion as a function of time t can be written as,

$$\frac{d\hat{\mathbf{v}}(t)}{dt} = \frac{qc^2}{E} \hat{\mathbf{v}} \times \mathbf{B}. \quad (2.7)$$

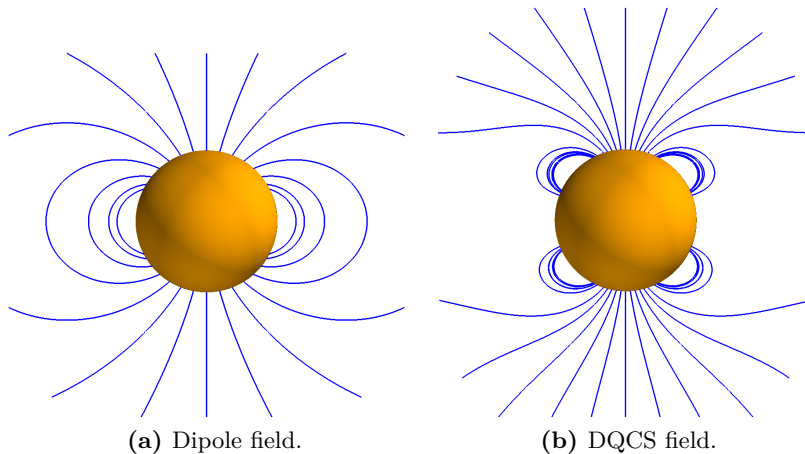


Figure 1. Magnetic field configuration models used in the simulation.

The direction of propagation of a particle after it traverses a distance Δs in time interval Δt can be approximated by using a Taylor series expansion of $\hat{\mathbf{v}}(t + \Delta t)$ around t ,

$$\hat{\mathbf{v}}(t + \Delta t) \approx \hat{\mathbf{v}}(t) + \frac{d\hat{\mathbf{v}}(t)}{dt} \Delta t,$$

which takes the form

$$\hat{\mathbf{v}}(t + \Delta t) \approx \hat{\mathbf{v}}(t) + \frac{qc^2}{E} (\hat{\mathbf{v}} \times \mathbf{B}) \Delta t, \quad (2.8)$$

after substituting $\frac{d\hat{\mathbf{v}}(t)}{dt}$ from eq. (2.7). We implement such a particle motion by choosing an appropriate Δs which is split into two halves each equal to $\Delta s/2$. In the first half of the time interval $\Delta t/2 = \Delta s/2c$, the particle is propagated with the current direction vector which is then updated using eq. (2.8) and is propagated with the new direction vector for the latter half of the interval.

Using an expression for the spectral distribution of energy radiated by ultra-relativistic electron from [21]

$$f(y) = \frac{9\sqrt{3}}{8\pi} \frac{y}{(1 + \xi y)^3} \left\{ \int_y^\infty K_{\frac{5}{3}}(z) dz + \frac{(\xi y)^2}{1 + \xi y} K_{\frac{2}{3}}(y) \right\}$$

where parameter $\xi = \frac{3}{2} \frac{H_\perp}{H_{\text{cr}}} \frac{E}{m_e c^2}$, E and m_e are energy and rest mass of electron respectively and y is a function of emitted photon energy $h\nu$ defined by

$$y(h\nu) = \frac{h\nu}{\xi(E - h\nu)},$$

one can obtain the probability of emission of a bremsstrahlung photon from a sufficiently small path length dl . As has been derived in [16], the probability can be written as

$$P_{\text{brem}}(B_\perp, E, h\nu, dl) = dl \int_0^E I(B_\perp, E, h\nu) \frac{d(h\nu)}{h\nu}, \quad (2.9)$$

with

$$I(B_{\perp}, E, h\nu) \equiv \frac{h\nu dN}{d(h\nu) dl},$$

where dN is the number of photons with energy between $h\nu$ and $h\nu + d(h\nu)$ emitted over the path length dl .

In addition, we have included the angular distribution of emitted synchrotron photons in our simulations. Since electrons are ultra-relativistic, we take the half-opening angle of emitted synchrotron photons to be equal to $1/\gamma$, γ being the Lorentz factor of the electron. The azimuthal angle of emitted photon is randomly chosen from a uniform distribution $U(0, 2\pi)$ [22].

3 Results

We performed simulations for various representative cases of primary UHE photons traversing the Sun's vicinity on their way towards the Earth. The solar magnetic field component transverse to the propagation direction of primary UHE photon has sufficiently large strength for pair production only in a small fraction of the path length close to the Sun. Emission of synchrotron photons from the e^+e^- pair produced in this way also occurs mostly in the region near to the Sun. Thus, almost the entire cascade development occurs in the close vicinity of the Sun.

The electron and the positron, although travelling along slightly different tracks, experience practically the same transverse magnetic field strength. The electron and the positron are deviated in opposite directions approximately in the same plane, when considered only in the small region where most of the cascade develops. The argument that their motion is approximately in the same plane comes from the fact that for the highly energetic e^+e^- travelling in a magnetic field of which the strength typically is much less than a Gauss, the gyroradius of the motion is much larger than the length of the track where they experience this field. Synchrotron photons emitted from these ultra-relativistic electrons are highly beamed in the forward direction of the latter, which gives rise to spatial distribution that has a very elongated footprint, when the cascade arrives at the top of the Earth's atmosphere. The probability of conversion of a 100 EeV UHE photon propagating towards the Earth from the Sun's vicinity as a function of its impact parameter is shown on figure 2 for equatorial and polar incidence. The conversion probability is close to unity for impact distance as far as $4R_{\odot}$ for equatorial incidence from the Sun's center for a 100 EeV photon, which translates to the fact that despite a small solid angle subtended by the Sun while viewed from the Earth, the effective solid angle relevant for SPS search is about 15 times larger at this energy. However, for lower energies around 10 EeV, the conversion probability is close to unity as far as $2R_{\odot}$, thus giving a region 3 times larger than the apparent size of the Sun viewed from the Earth. For the case when a primary photon traverses a region very close to the Sun ($\sim 1R_{\odot}$), conversion probability is close to 1 even for a 1 EeV photon. Similar conclusions apply to the photon polar incidence case, exhibiting slightly larger values for the corresponding impact parameter. Also, in figure 3, spatial distribution of photons for an example case is shown. In the plot, $y = 0, z = 0$ corresponds to the point at the top of the Earth's atmosphere where the UHE photon would have landed, had there been no interaction on its way. Positive y and z axes point towards the East and the North directions respectively. Although the particle distribution is dependent on the solar magnetic field model used in the simulation as is evident in the figure, the nature of the particle distribution (i.e., a very extended spatial

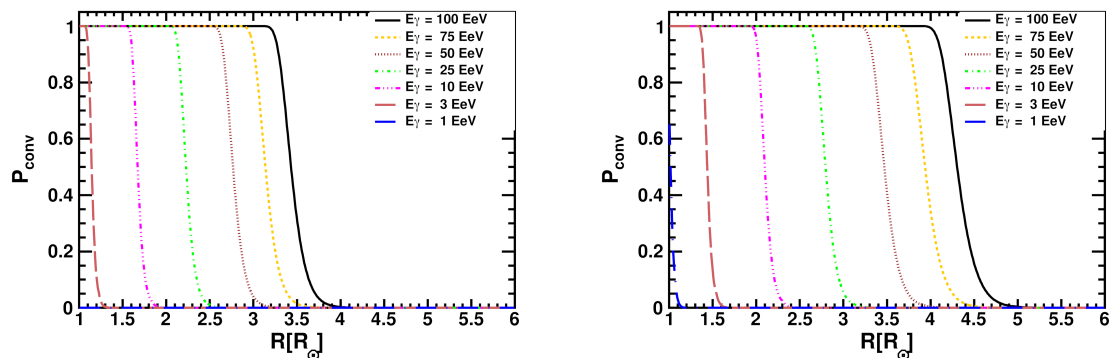


Figure 2. Probability of magnetic pair production ($\gamma \rightarrow e^+e^-$) as a function of the impact parameter for UHE photons heading towards the Earth from the Sun’s vicinity using the dipole magnetic field model. *Left panel:* equatorial photon incidence. *Right Panel:* polar photon incidence.

distribution) holds for both models. A salient feature of SPSs we observe in our simulation results is a very extended spatial distribution of cascade particles, apparently along a straight line, as the cascade reaches the top of the Earth’s atmosphere. This extended footprint is a straightforward consequence of the deviation of electrons and positrons along their tracks under the influence of (practically the same) solar magnetic field, and emission of highly forward-beamed synchrotron photons from them as they propagate towards the Earth. In figure 4, dipole model SPS footprint sizes for 50 and 100 EeV photons heading towards the Earth from different directions are shown. SPS footprint size in plots 3, 4, 5 is defined as the spatial extent of photons with energies of 1 MeV and higher on the plane distant from the Sun by 1 AU. The plots are obtained from 1000 simulations each with the impact position of photons heading towards the Earth randomly chosen from a uniform two dimensional distribution around the Sun such that the range of impact parameter is between $1R_\odot$ and $5R_\odot$. Figure 5 presents the results of both models for 0° and 45° latitudes. In figure 6, the particle distribution at the top of the Earth’s atmosphere weighted by particle energy for an example simulation is shown. The central region of the cascade comprises the most energetic photons. Figure 7 shows the corresponding energy distribution of photons in the SPS cascade displayed in the previous figure. An important implication of remarkably large sizes of SPSs demonstrated in figures 3, 4, and 5 is that SPS tails might reach Earth even if the primary UHE photons which initiate these SPSs arrive from the directions much different from the direction of the Sun, i.e., practically from the sky hemisphere with the Sun in its center.

3.1 Multi air shower footprints at the ground level

In order to demonstrate the capabilities of detection of multi air shower footprints on Earth, we have performed simulations of different geometrical configurations of ideal ground detectors. In order to derive a distribution of the of SPS-induced air shower particles on the surface of the Earth, simulations with the CORSIKA program [23] were performed. The multi air shower particle distributions were obtained taking as an input to CORSIKA the spatially extended SPS distributions generated with the modified PRESHOWER program, with several additional adjustments to keep the compatibility with CORSIKA. The resultant particle distributions form very characteristic, “galaxy-shaped” footprints composed of many extended air showers with significantly dispersed cores, as demonstrated with an example shown in fig-

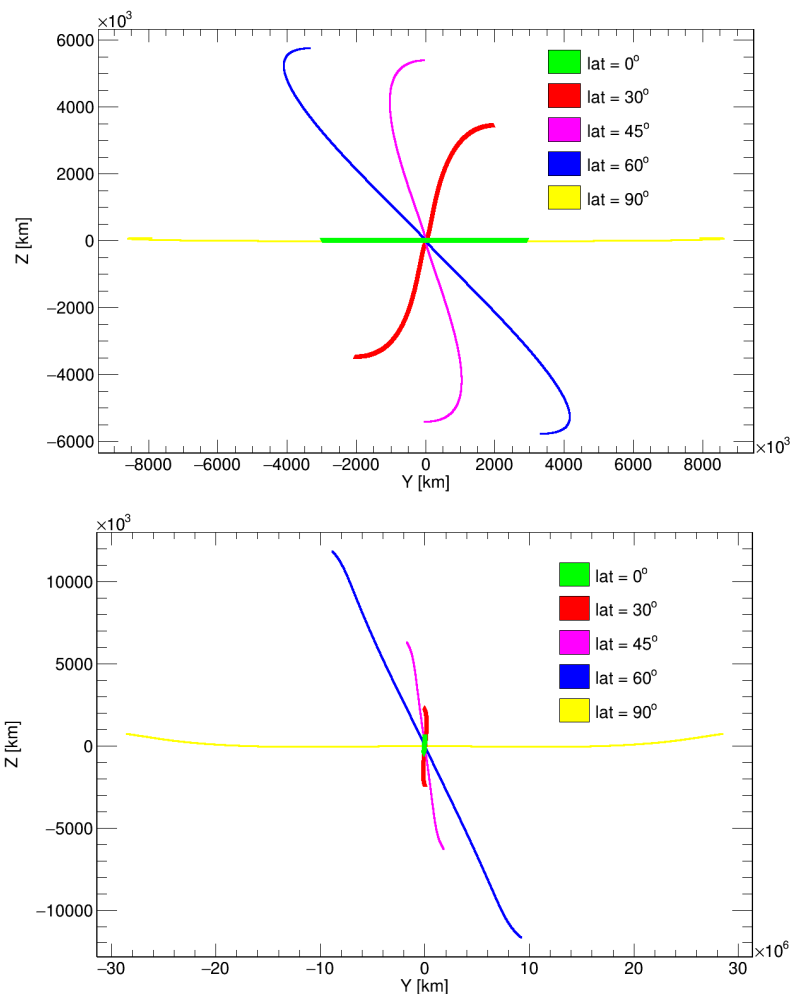


Figure 3. Spatial distribution of photons with energies $> 10^6$ eV arriving at the top of the atmosphere for an SPS produced by a 100 EeV photon. The primary photon is directed towards the Earth such that the position of the closest approach has several heliocentric latitudes: 0° , 30° , 45° , 60° , and 90° . The impact parameter is fixed with a value of $2R_\odot$. In the top panel, the presented distribution corresponds to the dipole model of the magnetic field of the Sun whereas the bottom panel displays the results for the DQCS model.

ure 8. By applying a simple geometrical study we demonstrate below that the SPS footprints are not only reconstructable, but that they can also be clearly distinguished from particle distributions typical of single EAS. Figure 9 qualitatively shows the detection capability of an example SPS footprint shape after applying several detector array configurations featuring variable single detector dimensions and positioning. We assume ideal conditions for detection: particle falling inside the planar box of the detector is detected with 100% efficiency. Within the figure, we keep the detector array size and spacing between individual detector units fixed while varying their sizes. It is clearly seen that the characteristic “galaxy-like” shapes of SPS footprints are reconstructable, although the required detector array parameters might be economically demanding. But even if a characteristic shape of the central regions of an SPS-induced particle distribution cannot be reconstructed, one can base the experimental strategies on observing air shower “walls”: groups of extensive air showers with

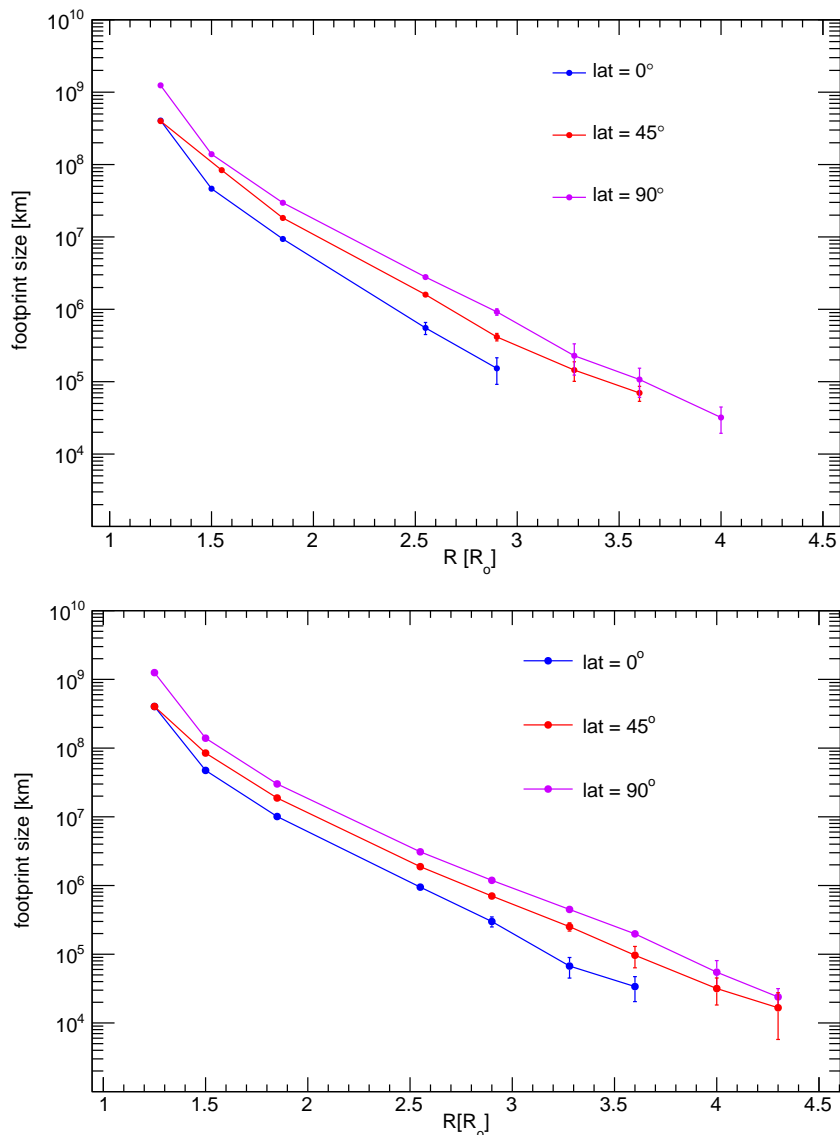


Figure 4. Size of SPS footprint at a distance of 1 AU from the Sun as a function of impact parameter R for a primary photon with an energy of 50 EeV (top panel) and 100 EeV (bottom panel). The SPS footprint size is defined as the spatial extent of photons with energies of 1 MeV and higher on the plane distant from the Sun by 1 AU. The values obtained in these plots correspond to the dipole magnetic field model of the Sun.

parallel axes, all practically contained within one plane. The projection of such a plane onto the Earth surface might span the whole hemispheres of the globe and provide very promising experimental opportunities. While a detailed planning of the relevant observational strategies requires a dedicated follow-up study which is still in progress, the qualitative picture presented in this report might serve as an argument in favor of the SPS detection feasibility, also in terms of the expected event rates. In fact, we can consider the flux from the Pierre Auger Observatory, i.e., upper limits of diffuse flux of UHE photons of energies above 10 EeV, $\phi_{\gamma}^{\text{diff}}(10 \text{ EeV}) \sim 2 \times 10^{-3} \text{ km}^{-2} \text{ yr}^{-1} \text{ sr}^{-1}$ [9] in order to estimate the fraction of events emitted from vicinity of the Sun where an SPS is likely to originate. By considering a ring of solid

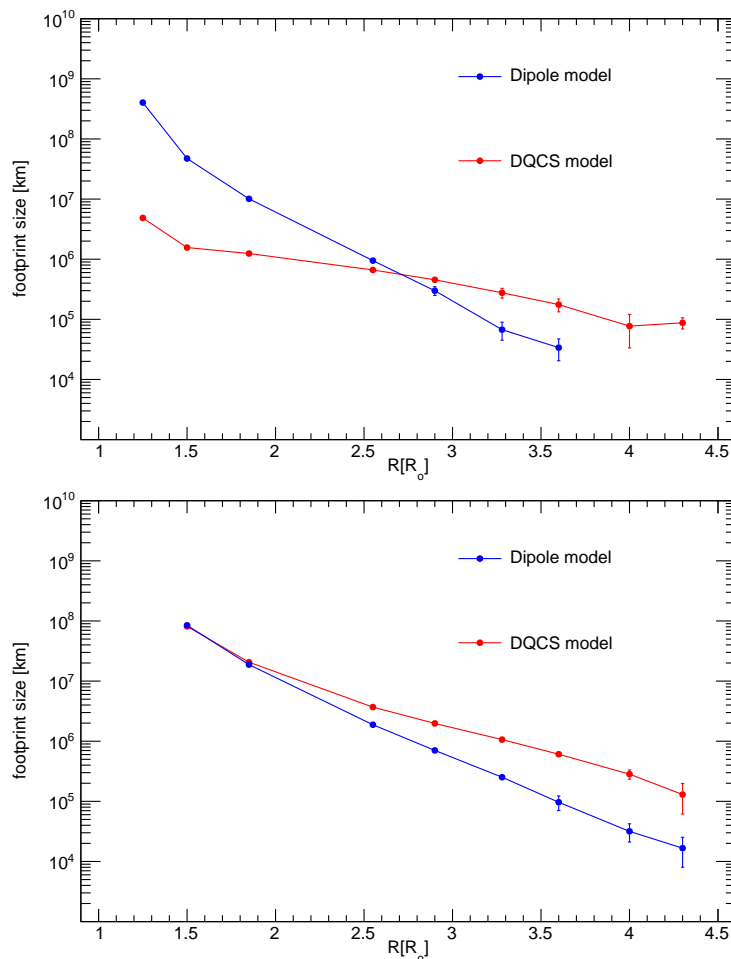


Figure 5. Size of footprint for the DQCS and Dipole Model as a function of impact parameter R for a primary photon with an energy of 100 EeV with a) latitude 0° (top panel) and b) latitude 45° (bottom panel). The SPS footprint size is defined as the spatial extent of photons with energies of 1 MeV and higher on the plane distant from the Sun by 1 AU.

angle with external radius of $R_{\text{ext}} = 2.5R_{\odot}$ optimal for magnetic pair production as displayed in figure 2, and internal radius $R_{\text{int}} = 1R_{\odot}$ with value of 3.5×10^{-4} sr, we can estimate for the Pierre Auger Observatory, whose effective area is of about 3000 km^2 and lifetime of about 30 years, a number of events of about $2 \times 10^{-3} \times 3.5 \times 10^{-4} \times 3000 \times 30 \sim 0.06$. This example event rate based on observational upper limits tells us about an *optimistic* (already non-negligible) chance for a new (unobserved) physics detection with the available infrastructure, if we assume that a specific characteristics (remarkable elongation of particle distribution) of SPSs makes them recognisable under ideal conditions for detection, and that the Pierre Auger Observatory or a detector array of a similar size can be tuned to be sensitive to SPSs with a reasonable efficiency. Furthermore, the expected SPS event rate might grow if a joint, multi-observatory analysis is being performed continuously, and if we consider a possible sensitivity to the groups of particles propagating far from SPS cores, in the tails extending even over many millions of kilometers (as seen in figures 3, 4, and 5), as it would increase the solid angle around the Sun from where an observable SPS could be expected. A characteristic spatial elongation of SPSs demonstrated above indicates that particle distributions of central

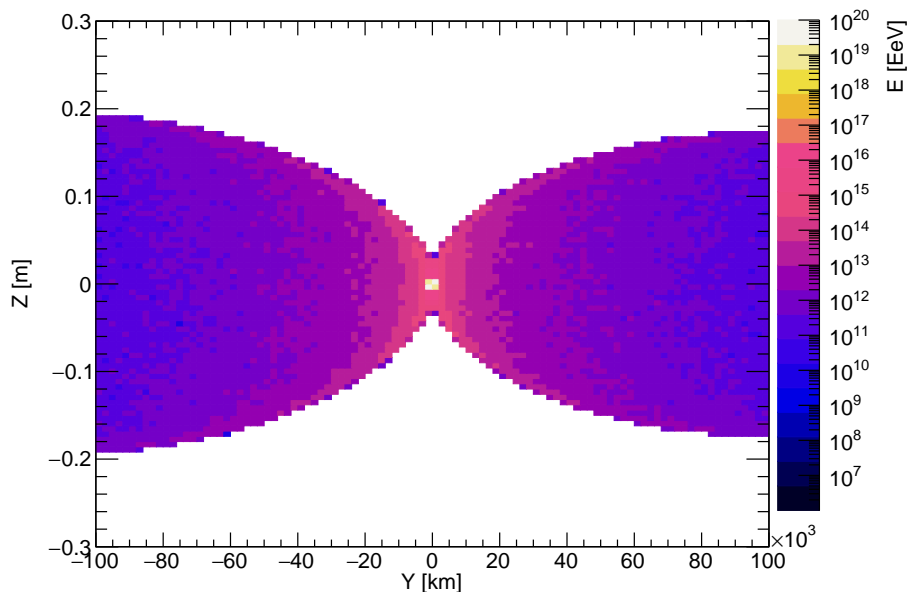


Figure 6. Distribution of energy of SPS photons arriving at the top of the atmosphere in a central region of an SPS produced by a 100 EeV photon. The primary photon is directed towards the Earth such that the position of the closest approach has heliocentric latitude 0° , and its impact parameter is $3R_\odot$. Note the difference in the scales along y and z axes.

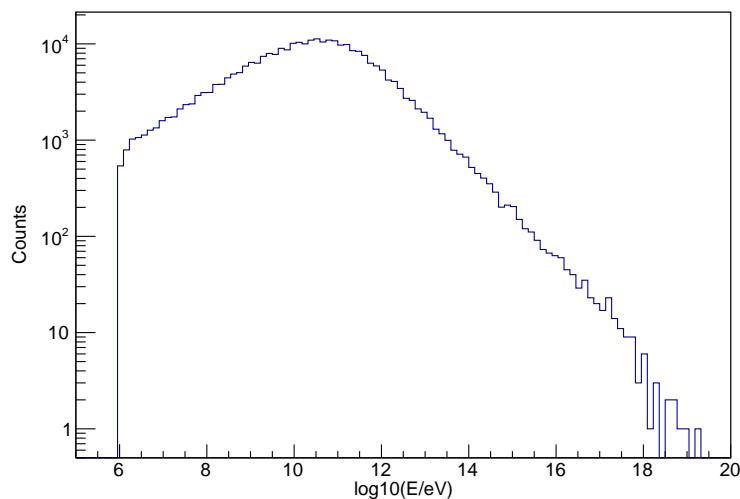


Figure 7. Energy distribution of SPS photons with energies larger than 10^6 eV for a SPS produced by a 100 EeV photon. Such a primary photon is directed towards the Earth and its impact parameter is $3R_\odot$.

parts of SPSs are very peculiar in comparison with single air shower footprints. In order to understand the topology of multi air shower footprints generated by SPSs, we then choose to characterize the corresponding particle distributions by comparing them to those induced by

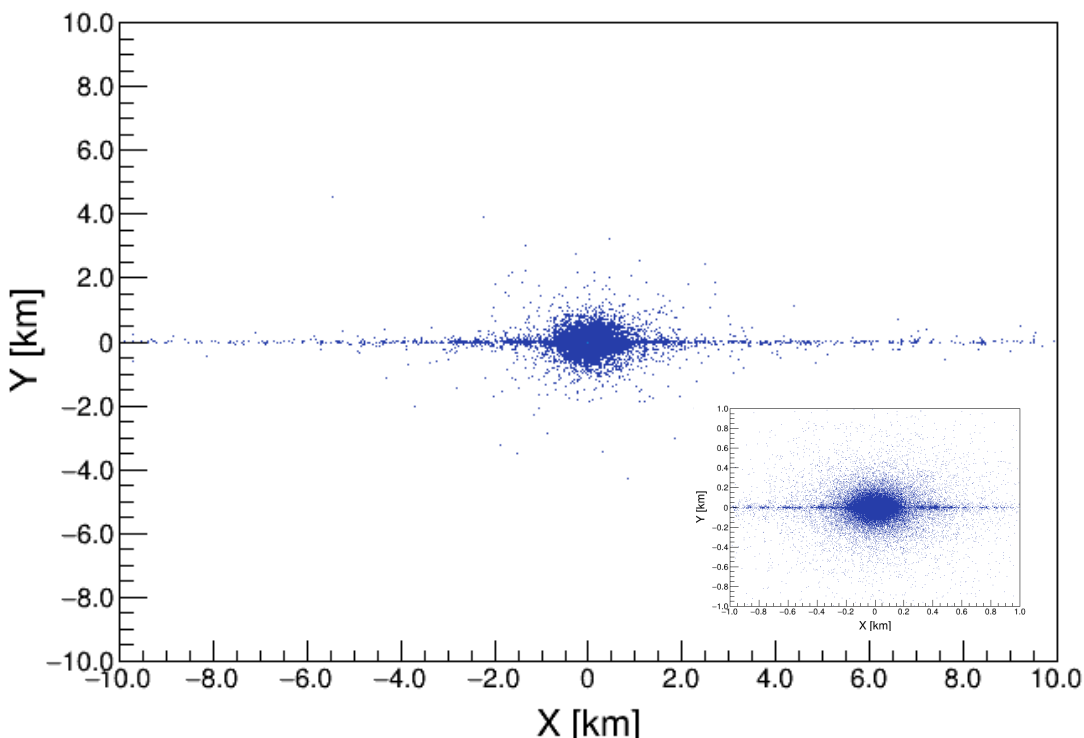


Figure 8. The central regions of an example multi air shower particle distribution on ground generated by an SPS originated from a primary UHE photon of energy 10^{19} eV. The inset displays the core of the footprint in a smaller area.

unconverted UHECR photons. The left panel of figure 10 presents the case of an individual air shower induced by a primary photon of energy 10^{19} eV, arriving vertically at the detector site. Here the black circle denotes the area containing 90% of secondary particles that comprise an air shower. On the other hand, as can be seen in the right panel of figure 10, the multi air shower footprint produced by an SPS generated by a photon of the same energy has a compact particle distribution around the cores of the central, most energetic showers accompanied by an extended, very thin area containing air showers of lower energies. We conclude that the elongated, “galaxy”-like shapes of the SPS-induced particle distributions on the ground are clearly distinguishable from the footprints of individual extensive air showers, and that the multi air shower particle distribution might potentially be observable under conditions of 100% detection efficiency due to the aforementioned characteristic pattern.

The ongoing follow-up studies dedicated to specific UHE photons scenarios, applying more realistic detector configurations, and involving more precise particle distributions will help to quantify the SPS event rate expectations and detection efficiencies attainable with particular infrastructure capabilities. One of the promising experimental initiatives within which relevant studies and the corresponding experimental efforts are being undertaken is the Cosmic Ray Extremely Distributed Observatory (CREDO) collaboration [17]. CREDO aims at the search for large scale cosmic ray correlations using the available and future data on cosmic and gamma ray events of energies that span the whole cosmic ray energy spectrum, and the results presented in this article contribute directly to the CREDO science program.

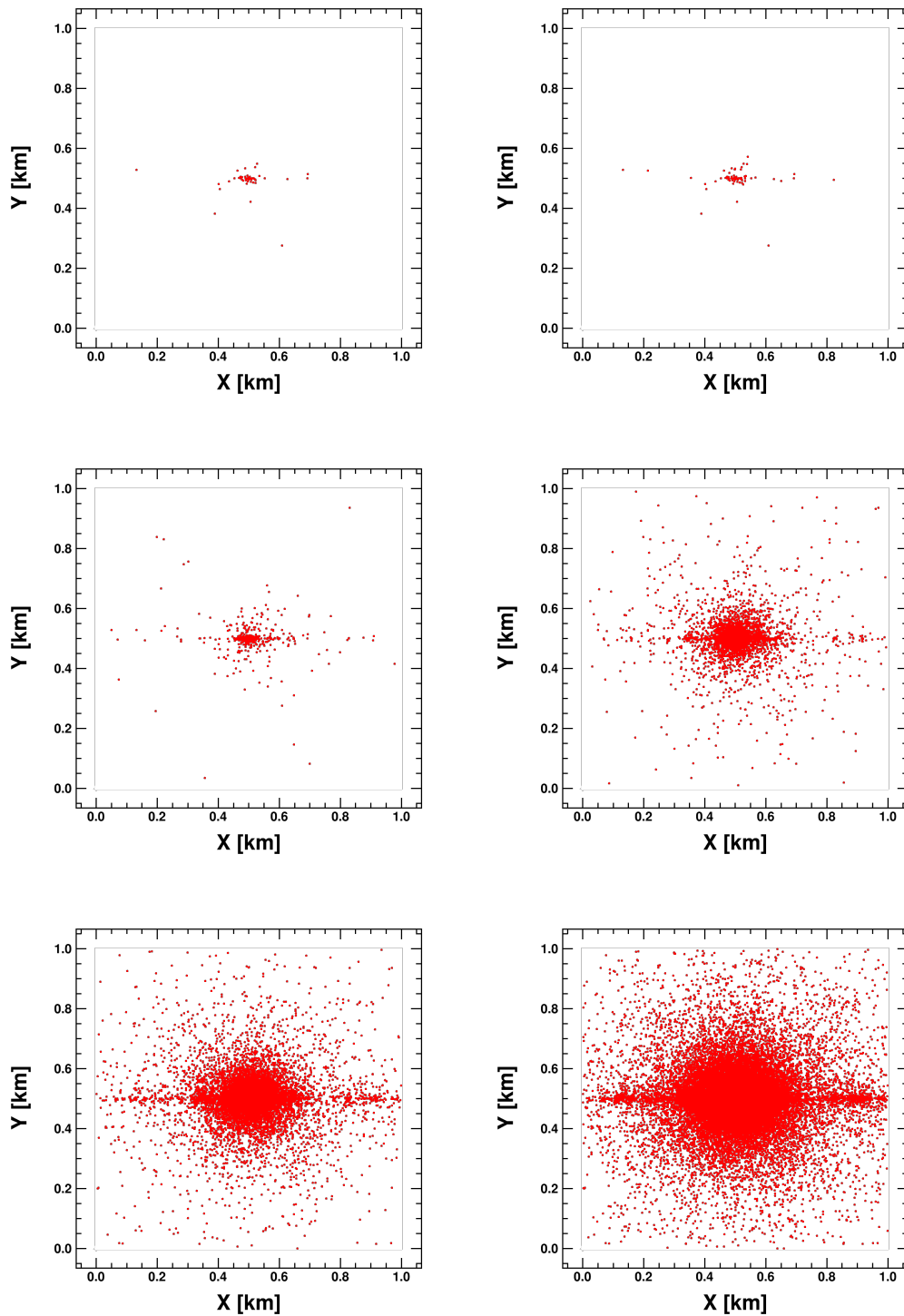


Figure 9. Detected footprint of an SPS generated by a 10^{19} eV photon by detector arrays of different geometries, all located on ground. All the figures share the same covered area which corresponds to 1 km^2 whereas the spacing between detector units is 25 cm. The single unit detector is presented as a square area. *Upper row:* detector area of 0.16 cm^2 (left) and 0.25 cm^2 (right). *Middle row:* detector area of 2 cm^2 (left) and 25 cm^2 (right). *Lower row:* detector area of 100 cm^2 (left) and 400 cm^2 (right).

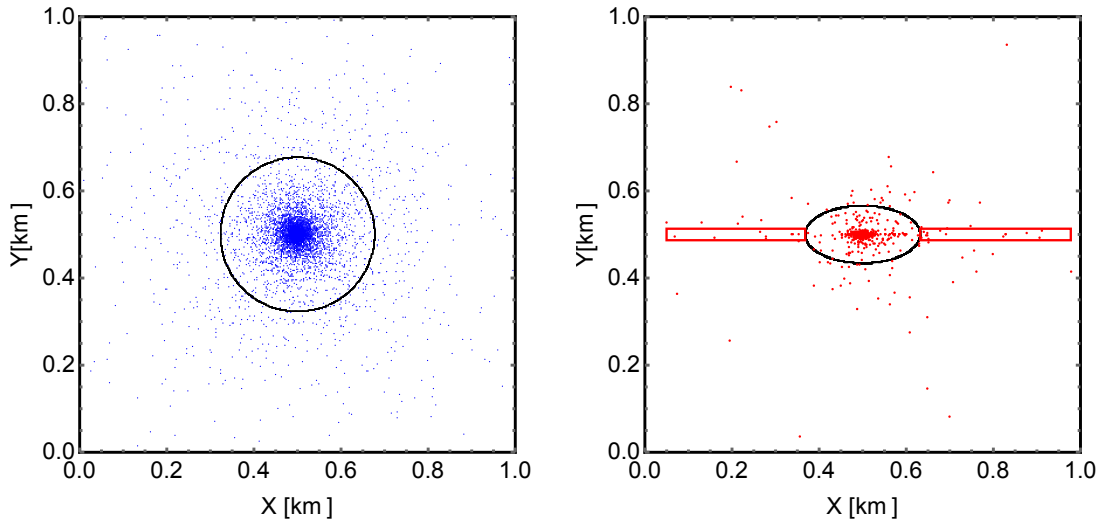


Figure 10. Footprints of an unconverted photon (left panel) and of an SPS (right panel), both of energies of 10 EeV, arriving vertically at the Earth, and detected on ground by an array of sensors, each of them with a collecting area of 2 cm^2 , all spaced by 25 cm (as in the left panel of the middle row in figure 9). The areas inside the black contours contain 90% of the particle distributions whereas the red rectangles on the right panel serve to guide the eye in order to highlight the part of the remaining detected particles within a rather extended distribution characteristic of the *galaxy-shape* footprint, as clearly seen in figure 9.

4 Summary and prospects

Our simulation results show that photons in SPS cascades are extended over a huge spatial extent (even millions of kilometers) practically along a line. The orientation and size of these line-like signatures, however, depend on the initial direction and impact position of the primary UHE photon relative to the solar magnetic field. Also, photons in SPS cascades can possess energies that span more or less the whole cosmic-ray energy spectrum, from below GeV to above an EeV.

Detection of SPS cascades is limited by two major requirements. The first is the size of the detector itself, which should be big enough to detect SPS particles distributed over very large distances. The other obvious requirement is that the detector should be operational during the daytime. As such, only a large array of ground-based particle detectors like the Pierre Auger Observatory [24] would be suitable for SPS detection. However, the most promising experimental approach to SPS observation and studies should go even further to form a global alliance of all radiation detector arrays and individual sensors capable of detecting secondary particles from the extensive air showers produced by SPSs. Such an alliance is envisaged by the (CREDO) experiment [17].

Given the current UHE photon limits [9, 25, 26], the expected number of SPSs with cores landing within an observatory of the size of Auger is small, although non-negligible. Our result of 0.002 events per year from optimistic consideration of the upper limits of the surface of the Pierre Auger Observatory demonstrate how challenging it can be to detect these small fluxes. Nevertheless, the characteristic footprint shapes are definitely unmistakable. A multi-collaboration SPS observation campaign, as well as the sensitivity of a detector network to the tails of the significantly elongated SPSs allows expecting an experimentally interesting rate of events arriving from a considerably large region of the sky, not only from a region around the Sun.

SPS-like processes at other sites in the Universe as well as other physics processes might also produce a “shower” of correlated particles, the cosmic ray ensembles (CREs), while they propagate in space. Thus, other stellar objects which have a magnetic field strength at least of the order of 0.1 G at their surfaces will also initiate SPS-like CREs. If we assume that a UHE photon undergoes an SPS-like process in regions of the Universe with relatively stronger magnetic field while heading towards the Earth and we have a cosmic ray detection framework that can detect two or more photons simultaneously at very distant locations, the “explorable horizon” for such process can be estimated using simple geometry considerations. From our SPS simulation results for 100 EeV photon, minimum distances between the most energetic (> 1 EeV), and low energy (1–10 TeV) SPS photons as the cascade reaches the top of the Earth’s atmosphere are both of the order of the order of 0.001 m. Provided a framework which can detect these “close photons” in the CREs arriving as far as 10 000 km apart at the Earth from extragalactic regions or sites, the “horizon” is extended to ~ 100 kpc, i.e. roughly to the size of our Galaxy. For comparison, the mean free path for gamma-rays at 1 EeV (1 TeV) is of the order of 100 kpc (500 Mpc). Interestingly, the study presented in [27] shows another mechanism of cosmic ray emission near the Sun, through the interaction of photons from the Sun with nearby cosmic-rays. This leads to more energetic excitations, such as Δ^+ production, which can lead to high-energy photons from π^0 decays, muons from charged pion decays, and neutrons. Even though not featuring the galaxy shape footprint, the predicted photon flux is of about the same order of magnitude as the predictions of our study.

Photon splitting in strong magnetic fields in the proximity of neutron stars [28, 29] is another process which is capable of producing CREs, of which the estimation of the expected signature at the Earth requires a dedicated study and will be performed in the near future. Although we are not certain about the expected rate of CREs, these, together with SPSs constitute a yet-unchecked scenario that is easy to verify and has a potential of opening a new window to the Universe.

Acknowledgments

This work was partly funded by the International Visegrad Fund Grant No. 21720040 and 21920298 and by the National Science Centre Grants No. 2016/23/B/ST9/01635 and 2020/39/B/ST9/01398. This research has also been supported in part by PLGrid Infrastructure. We warmly thank the staff at ACC Cyfronet AGH-UST, for their always helpful supercomputing support. CREDO mobile application was developed in Cracow University of Technology. K.Rz. acknowledges that his work was supported by the AGH University of Science and Technology in the year 2021 as research project No. 16.16.120.773. D.A-C. acknowledges support from the Bogoliubov-Infeld program for collaboration between JINR and Polish Institutions as well as from the COST actions CA15213 (THOR) and CA16214 (PHAROS). The work of J.Z-S. was funded by ANID-Millennium Science Initiative Program — ICN2019_044. N.D. acknowledges support from Tribhuvan University through grant HERP DLI-7B.

References

- [1] XENON100 collaboration, *Dark Matter Results from 100 Live Days of XENON100 Data*, *Phys. Rev. Lett.* **107** (2011) 131302 [[arXiv:1104.2549](#)] [[INSPIRE](#)].
- [2] CDMS-II collaboration, *Dark Matter Search Results from the CDMS II Experiment*, *Science* **327** (2010) 1619 [[arXiv:0912.3592](#)] [[INSPIRE](#)].

- [3] LUX collaboration, *First results from the LUX dark matter experiment at the Sanford Underground Research Facility*, *Phys. Rev. Lett.* **112** (2014) 091303 [[arXiv:1310.8214](#)] [[INSPIRE](#)].
- [4] M. Garny, M. Sandora and M.S. Sloth, *Planckian Interacting Massive Particles as Dark Matter*, *Phys. Rev. Lett.* **116** (2016) 101302 [[arXiv:1511.03278](#)] [[INSPIRE](#)].
- [5] R. Aloisio, S. Matarrese and A.V. Olinto, *Super Heavy Dark Matter in light of BICEP2, Planck and Ultra High Energy Cosmic Rays Observations*, *JCAP* **08** (2015) 024 [[arXiv:1504.01319](#)] [[INSPIRE](#)].
- [6] P. Bhattacharjee and G. Sigl, *Origin and propagation of extremely high-energy cosmic rays*, *Phys. Rept.* **327** (2000) 109 [[astro-ph/9811011](#)] [[INSPIRE](#)].
- [7] K. Greisen, *End to the cosmic ray spectrum?*, *Phys. Rev. Lett.* **16** (1966) 748 [[INSPIRE](#)].
- [8] G.T. Zatsepin and V.A. Kuzmin, *Upper limit of the spectrum of cosmic rays*, *JETP Lett.* **4** (1966) 78 [*Pisma Zh. Eksp. Teor. Fiz.* **4** (1966) 114] [[INSPIRE](#)].
- [9] PIERRE AUGER collaboration, *A search for ultra-high-energy photons at the Pierre Auger Observatory exploiting air-shower universality*, *PoS ICRC2021* (2021) 373 [[INSPIRE](#)].
- [10] PIERRE AUGER collaboration, *Limits on ultra-high energy photons with the Pierre Auger Observatory*, *PoS ICRC2019* (2021) 398 [[INSPIRE](#)].
- [11] PIERRE AUGER collaboration, *Upper limit on the cosmic-ray photon fraction at EeV energies from the Pierre Auger Observatory*, *Astropart. Phys.* **31** (2009) 399 [[arXiv:0903.1127](#)] [[INSPIRE](#)].
- [12] PIERRE AUGER collaboration, *Upper limit on the cosmic-ray photon flux above 10^{19} eV using the surface detector of the Pierre Auger Observatory*, *Astropart. Phys.* **29** (2008) 243 [[arXiv:0712.1147](#)] [[INSPIRE](#)].
- [13] TELESCOPE ARRAY collaboration, *Study of muons from ultrahigh energy cosmic ray air showers measured with the Telescope Array experiment*, *Phys. Rev. D* **98** (2018) 022002 [[arXiv:1804.03877](#)] [[INSPIRE](#)].
- [14] PIERRE AUGER collaboration, *Muons in Air Showers at the Pierre Auger Observatory: Mean Number in Highly Inclined Events*, *Phys. Rev. D* **91** (2015) 032003 [*Erratum ibid.* **91** (2015) 059901] [[arXiv:1408.1421](#)] [[INSPIRE](#)].
- [15] W. Bednarek, *Cascades initiated by EHE photons in the magnetic field of the earth and the sun*, [astro-ph/9911266](#) [[INSPIRE](#)].
- [16] P. Homola et al., *Simulation of ultrahigh energy photon propagation in the geomagnetic field*, *Comput. Phys. Commun.* **173** (2005) 71 [[astro-ph/0311442](#)] [[INSPIRE](#)].
- [17] CREDO collaboration, *Cosmic Ray Extremely Distributed Observatory*, *Symmetry* **12** (2020) 1835 [[arXiv:2010.08351](#)] [[INSPIRE](#)].
- [18] T. Erber, *High-energy electromagnetic conversion processes in intense magnetic fields*, *Rev. Mod. Phys.* **38** (1966) 626 [[INSPIRE](#)].
- [19] J.K. Daugherty and A.K. Harding, *Pair production in superstrong magnetic fields*, *Astrophys. J.* **273** (1983) 761 [[INSPIRE](#)].
- [20] M. Banaszekiewicz, W.I. Axford and J.F. McKenzie, *An analytic solar magnetic field model*, *Astron. Astrophys.* **337** (1998) 940.
- [21] A.A. Sokolov and I.M. Ternov, *Radiation from Relativistic Electrons*, in *AIP Translation Series*, AIP, New York NY U.S.A. (1986).
- [22] N. Dhital et al., *Simulation of ultra-high energy photon propagation with PRESHOWER 3.0*, submitted to *Comput. Phys. Commun.*, in preparation.

- [23] D. Heck, J. Knapp, J.N. Capdevielle, G. Schatz and T. Thouw, *CORSIKA: A Monte Carlo code to simulate extensive air showers*, FZKA-6019 (1998) [[INSPIRE](#)].
- [24] PIERRE AUGER collaboration, *The Pierre Auger Cosmic Ray Observatory*, *Nucl. Instrum. Meth. A* **798** (2015) 172 [[arXiv:1502.01323](#)] [[INSPIRE](#)].
- [25] PIERRE AUGER collaboration, *A targeted search for point sources of EeV photons with the Pierre Auger Observatory*, *Astrophys. J. Lett.* **837** (2017) L25 [[arXiv:1612.04155](#)] [[INSPIRE](#)].
- [26] TELESCOPE ARRAY collaboration, *Search for point sources of ultra-high-energy photons with the Telescope Array surface detector*, *Mon. Not. Roy. Astron. Soc.* **492** (2020) 3984 [[INSPIRE](#)].
- [27] K.K. Andersen and S.R. Klein, *High energy cosmic-ray interactions with particles from the Sun*, *Phys. Rev. D* **83** (2011) 103519 [[arXiv:1103.5090](#)] [[INSPIRE](#)].
- [28] S.L. Adler, *Photon splitting and photon dispersion in a strong magnetic field*, *Ann. Phys.* **67** (1971) 599.
- [29] A.K. Harding, M.G. Baring and P.L. Gonthier, *Photon splitting cascades in gamma-ray pulsars and the spectrum of PSR 1509-58*, *Astrophys. J.* **476** (1997) 246 [[astro-ph/9609167](#)] [[INSPIRE](#)].